Inverting for reservoir pressure change using time-lapse time strain: Application to Genesis Field, Gulf of Mexico

Neil Hodgson and Colin MacBeth, Heriot-Watt University, Edinburgh, UK
Luca Duranti, James Rickett, and Kurt Nihei, Chevron ETC, San Ramon, California, USA

There are increasing numbers of published examples from around the world in which significant 4D time shifts have been observed in the overburden above producing reservoirs.

Indeed, this topic prompted the *TLE* special section "Rocks under strain" in December 2005. The significance of these 4D observations is that, if we wish to fully understand the 4D signature of compacting reservoirs, we can no longer think of the reservoir in isolation. The seismic response outside the reservoir changes because the nonreservoir rocks deform in response to reservoir activity. While these nonreservoir 4D seismic changes can obscure or contribute to the reservoir-level signal, making the 4D interpretation uncertain, if utilized appropriately they may also be used to provide information on the actual reservoir pressure changes. This new pressure information can thus be used to complement well measurements or other 4D seismic-based methods (such as the multi-attribute pressure and saturation inversion outlined by Floricich et al., 2006), providing valuable data for reservoir monitoring and management. In this paper, we build on the work of several authors who have presented methods to invert surface deformation measurements for reservoir volume or pressure change. We show how 4D seismic can extend this approach by focusing on the inversion of 3D strain deformation estimates for the overburden derived directly from the repeated seismic data. The method is then applied to Genesis Field in the Gulf of Mexico, in which there are series of compacting unconsolidated stacked turbidite reservoirs.

Time-lapse time strain. Rock velocities are sensitive to changes in stress and strain so that if a volume of rock strains, the change in traveltime through it will be made up of a contribution due to the change in distance traveled by the seismic wave and a contribution due to the change in velocity. A perturbation formula relating changes in vertical traveltime t, velocity v, and vertical layer thickness z, assuming small changes in thickness and velocity, is given by Landrø and Stammeijer (2004)

$$\frac{\Delta t}{t} = \frac{\Delta z}{z} - \frac{\Delta v}{v} \tag{1}$$

Hatchell and Bourne (2006) went on to make the assumption that changes in thickness and velocity can be linearly related by a constant of proportionality, R, which relates the fractional change in velocity and vertical strain so that $\Delta v/v = -R\varepsilon_{zz}$, resulting in the following relationship

$$\Delta t / t = (1 + R)\,\varepsilon_{zz} \tag{2}$$

where we have replaced $\Delta z/z$ by ε_{zz}, signifying the vertical component of the strain tensor. The left side of Equation 2 is the derivative of the time-shift field, which we term *time strain*. A method to obtain time-lapse time strains from 4D seismic is described in the companion paper in this special section ("4D time strain and the seismic signature of geomechanical compaction at Genesis"). If we have knowledge of the magnitude of R, we can obtain estimates of vertical strain directly from 4D seismic observations.

With estimates of vertical strain for the overburden, a linearized inversion can be employed to obtain reservoir pressure change. Segall (1992) shows that the displacement in a poroelastic medium can be given by the distribution of centers of dilatation with a magnitude proportional to $\alpha\Delta p(x,t)$. The i^{th} component of the displacement tensor u_i at an observation point x in the subsurface is given by

$$u_i(\boldsymbol{x},t) = \frac{\alpha}{\mu}\int_v \Delta p(\xi,t)\, g_i(\boldsymbol{x},\xi)\, dV_\xi \tag{3}$$

where α is Biot's coefficient, μ the shear modulus, Δp is the change in pore pressure, $\xi=(\xi_1,\xi_2,\xi_3)$ are the integration coordinates over the volume V, and $g_i(x,\xi)$ is the Green's function. We consider the pressure at two discrete times so that the time t in Equation 3 is irrelevant. Using Equation 3, we can calculate the displacement due to the pressure change in the whole reservoir by using a superposition of N elements of volume V_k, which undergo a pressure change Δp_k. The strain is found by differentiating the displacement Green's function.

$$\frac{\partial u_i}{\partial x_j} = \frac{\alpha}{\mu}\sum_{k=1}^{N}\Delta p_k \int_{V_k}\frac{\partial g_i(\boldsymbol{x},\xi)}{\partial x_j}\, dV_k \tag{4}$$

The Green's function in Equation 4 could be calculated in various ways. There is a trade-off between the advantages of simple solutions, such as the nucleus of strain method for a homogeneous elastic whole-space or half-space (Geertsma, 1966), which are easy to implement, computationally fast and require less parameterization, and the complexity of more sophisticated techniques, such as finite-element methods, which require a greater number of parameters and are computationally expensive. Note that while complex numerical methods such as finite-element modeling may correctly capture some degree of the Earth's heterogeneity, the misparameterization of such models could give misleading results.

The Green's function we adopt is the solution for a nucleus of strain in homogenous elastic half-space given by Geertsma. (For more details of the Green's function calculation, see Box 1). It should be noted that the elastic properties of the reservoir and overburden are assumed to be identical in this approach.

In practice, we can write Equation 4 as a linear system of equations. First the Green's function integral is precomputed to form a matrix of coefficients **G**, which describes the strain at a given subsurface observation point due to a unit pressure change in a reservoir volume V. This gives a linear matrix equation of the form

$$\varepsilon_{zz,M} = \sum_{n=1}^{N}\Delta p_n G_{n.M} = \Delta\mathbf{p}\mathbf{G} \tag{5}$$

where $\varepsilon_{zz,M}$ is the M^{th} observation given by Equation 2, and Δp are our unknown reservoir pressure changes. For geomodeling, a convenient subvolume out of which the reservoir can be constructed is a set of nonoverlapping cuboids.

The change in pressure is therefore an average change in pressure over each cuboid and the volume integral in Equation 5 is taken over the volume of each cuboid. Figure 1 gives a pictorial representation of how Equation 5 is applied for a rectangular reservoir split into four cuboids. To complement our strain observations we can add additional constraints to the inversion, such as hard constraints provided by engineering data (e.g., well-based pressure measurements) and soft constraints, preferring a smooth solution for example. We discuss this more in the following section. An overview of the entire workflow is given in Figure 2.

Application to Genesis Field. Hudson et al. (2006) give a comprehensive overview of the 4D project at Genesis. The field consists of turbidite reservoirs lying between 3000 and 5000 m. We concentrate on the three main producing intervals, the N1, N2, and N3L sands, which have average thicknesses of 21, 14, and 20 m, respectively. These are unconsolidated Lower Pleistocene-aged sands with initially high porosities of between 23 and 32% and high permeability of between 600 and 900 mD. The field has been depleted significantly and sands have undergone substantial compaction since first oil in 1999; furthermore, several wells have been lost due to compaction-related shear failure. The monitor survey was acquired in 2001, with the same orientation as the baseline. The two surveys were carefully coprocessed and cross-equalized to maximize repeatability (Magesan et al., 2005). Large time shifts are observed in the data in both reservoir and nonreservoir zones. Figure 3 shows the structure of the top N1 sand, upon which the time shifts have been superimposed. The majority of the time shift can be attributed to velocity reduction in the overburden due to overburden dilation, with a small contribution due to the subsidence where compaction has occurred. The time-shifts volume was converted to time strains, and then the time strains are further depth-converted using a velocity model, ready for input into the inversion.

To convert the time strain into strain we need to assign a value to the R factor (Equation 2). Hatchell and Bourne suggest that using R=5 for all nonreservoir rocks gives the optimal match between predicted and observed time shifts for several worldwide field examples. We adopt the same assumption that R is constant throughout the overburden. In the general case, however, the changes in velocity are likely to be anisotropic and R is likely to depend on the lithology and initial stress state (Holt et al., 2005). Uncertainty is especially a problem for overburden shales, whose geomechanical properties are, in general, less studied and more uncertain than reservoir rocks. We use another approach to estimate R. Equation 4 allows us not only to invert strains but also to forward model them, for known pressure changes. By using depletion estimates from the reservoir simulator, we can forward model strains and compare them to the observed time strains and calculate an average value for R via Equation 2. While the forward-modeled strains may be inaccurate, because the simulator input is only our current best estimate, unless it is wildly different from the real depletion field, it allows an order-of-magnitude calculation for R. For the Genesis overburden, we find R to be in the range of 6 ± 2, which is in keeping with Hatchell and

Box 1. The nucleus of strain concept for a homogeneous half-space.

The nucleus of strain concept can be used to provide the displacement field around a volume of reduced pore pressure (Δp) in homogeneous elastic half-space with a traction-free surface. A solution to the problem was first presented independently by Mindlen and Chen (1950) and Sen (1951) within the framework of thermoelasticity. Geertsma (1966) used this solution to provide analytical expressions for surface subsidence due to the depletion of a disc-shaped reservoir. The more general approach, for any reservoir geometry, is to sum the contributions due to volume elements that make up the reservoir. For practical applications the most convenient element is a cuboid. The general expression for displacement at the radical distance r and depth z due to an infinitesimal nucleus of strain located at (0,0,c) is given by

$$u = \frac{C_m}{4\pi}\left[\frac{\vec{S}}{S^3} + \frac{(3-4\nu)S_i}{S_i^3} - \frac{6z(z+c)\vec{S}_i}{S_i^3} - \frac{2\vec{k}}{S_i}\left\{(3-4\nu)(z+c) - z\right\}\right] \quad (1)$$

where $S = [r^2 + (z - c)^2]^{1/2}$ and $S_i = [r^2 + (z + c)^2]^{1/2}$. We take the vertical derivative of the above expression for vertical displacement given in that paper to obtain the vertical component of strain.

$$\varepsilon_{zz} = \frac{C_m}{4\pi}\left[\frac{1}{S^3} - \frac{3(z-c)^2}{S^5} + \frac{4\upsilon - 1}{S_i^3} + \frac{3(z+c)(4\upsilon(z+c) - (z-3c))}{S_i^5} - 6\left\{\frac{(z+c)^2}{S_i^5} + \frac{2z(z+c)}{S_i^5} - \frac{5z(z+c)^2}{S_i^7}\right\}\right] \quad (2)$$

To find the displacement or strain due to a cuboid the expressions must be integrated over the volume of the cuboid. The geometry applicable to the above equations is shown in Figure B1.

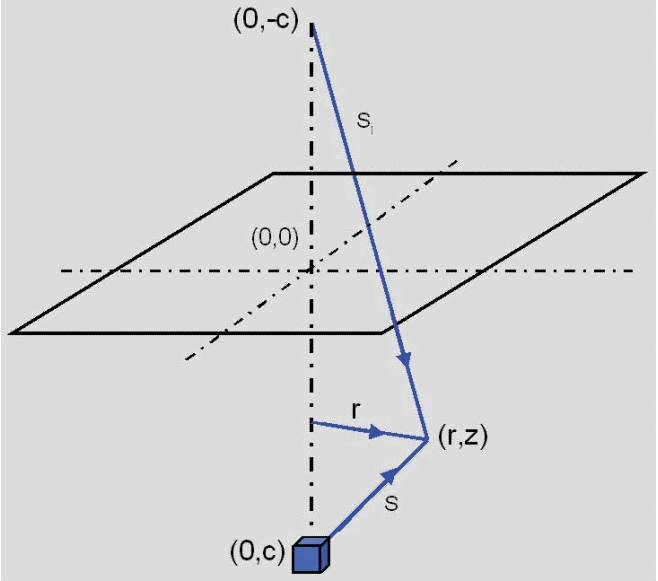

Figure B1. *The geometry to which Equation 5 is applied. Note that Geertsma uses z positive downward.*

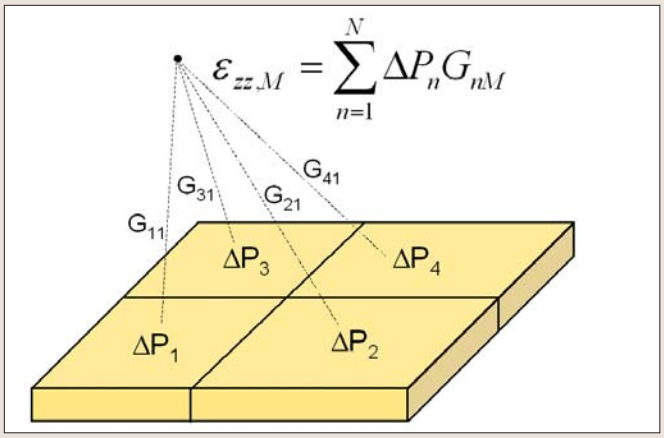

Figure 1. *A pictorial representation of Equation 5 for a rectangular reservoir split into four cuboids. The pressure change in each cube contributes to the observed strain.*

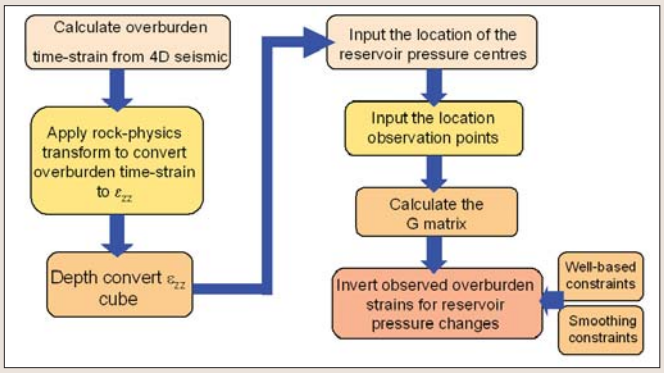

Figure 2. *The workflow to invert overburden time-lapse time strain for reservoir pressure depletion.*

Bourne's observations. An average of the overburden mechanical properties, which are derived from log data using empirical relationships for the dynamic to static transformation, and core data is used to define the mechanical properties of the half-space. The overburden properties are generally slowly varying, justifying this approach, with the exception of the wet Illinoisan sands, which are identified by Rickett et al. (2007) as possibly showing greater dilation than the surrounding shales.

Depletion upscaling and results. Synthetic modeling has shown that the inversion is stable where the reservoir is confined to a single layer. However, a problem arises when attempting to resolve closely spaced vertical layers; there may be a trade-off between pressure changes in layers at different depths. As the average vertical extent of the N series sands (including intersand shale) is not more than 80 m (see Figure 4 for a typical Genesis log), we take the practical approach of creating a single equivalent unit representing the three sand units. The equivalent unit is split into a regular grid composed of 114×46 cuboids of dimension $100\times100\times T$ meters, where T is the combined thickness of the three sands at any given location. The depth of the center of the unit is the average depth of the centers of each of the three individual units. This approach assumes insignificant interlayer geomechanical interaction (e.g., dilation of the inter-reservoir shales).

For noisy data, using as many observations as possible helps to ensure the robustness of the inversion solution. When choosing the number of data points, we are limited only by the spatial sampling interval of the time-strain volume and by the computational power needed to solve the large matrix equation (Equation 5). We use data from nine horizons in the overburden, separated by 200 m vertically on a grid 150×150 m (approximately 7000 data points). Equation 5 is solved using a least squares objective function with a smoothing constraint (using a Laplacian finite-difference operator) and constraining all areas with $NTG = 0$ to have zero pressure change. We also constrain the inversion using pressure data from seven major producing wells. A calibration of the inverted pressure change against well data is also required because the model assumes that the reservoir and overburden mechanical properties are identical, which can lead to underestimates of the reservoir pressure. In practice, the contrast between the reservoir and overburden materials will play a factor in the correct prediction of reservoir pressure, as discussed by Sayers et al. (2006).

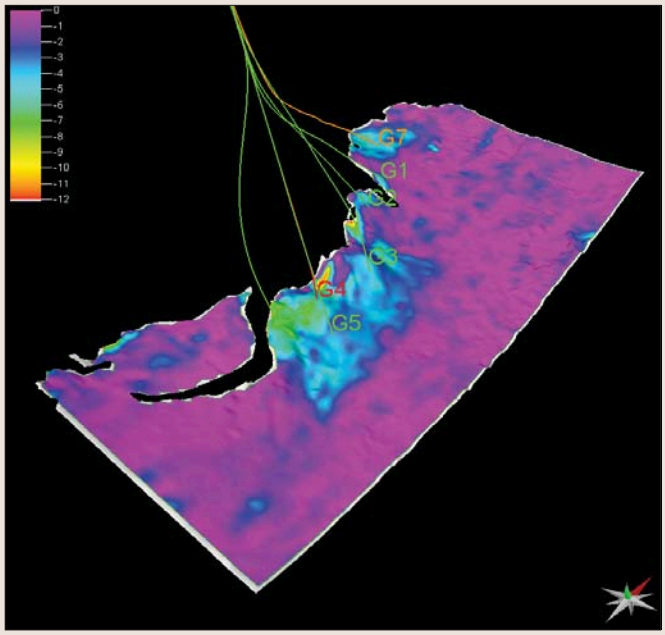

Figure 3. *Time shifts at the top of the first producing interval and giving an outline of the field. Time shifts show good correlation with producing wells. The majority of the time shift can be attributed to velocity reduction in the overburden due to overburden dilation. The color scale runs between 0 and –12 ms.*

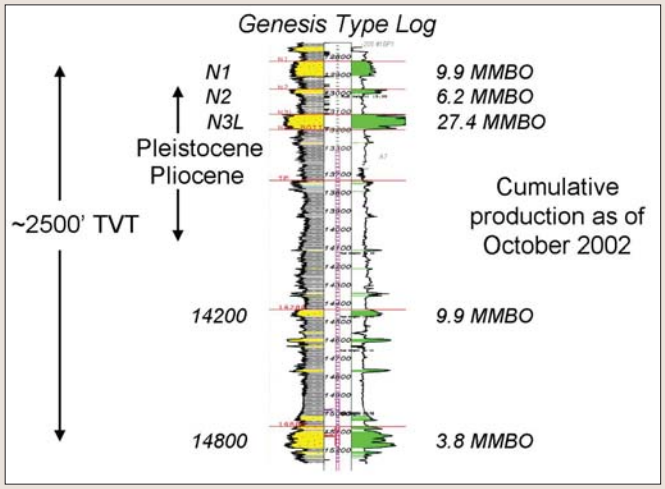

Figure 4. *A typical Genesis log. We are focusing on the three topmost producing intervals, which between them span no more than 80 m vertically (including intrareservoir shales).*

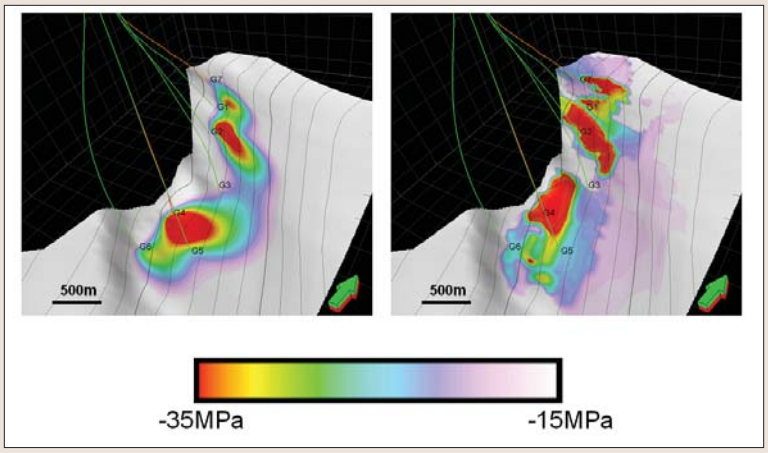

Figure 5. *Results from the inversion (left) compared with the reservoir simulator predictions (right). Color scale is between –15 and –32.5 MPa.*

We compare the inverted pressure depletion with a map determined using reservoir simulator predictions (Figure 5). The equivalent pressure map from the simulator shown is determined by taking the arithmetic sum of the pressure change over each of the intervals, which again assumes no significant geomechanical response of the inter-reservoir shales due to the reservoir depletion.

The agreement between the two maps is favorable. Although differing in fine-scale detail, the inversion correctly recovers the long wavelength features of the pressure distribution. Around well G4, the pressure change predicted by the simulator is oriented NS, while the inverted pressure lies EW. Also, in the north, the inverted depletion estimate is considerably less than that obtained from the reservoir simulator predictions. This latter observation is consistent with the findings of Rickett et al. (2007) which suggest that there may be an opportunity for infill drilling in this area. As expected, the inverted pressure is much smoother than the composite simulation prediction. This is partly due to our smoothness constraint, but it may also be related to the ultimate limit of resolution given the nature of the data that the time-lapse time-strain cubes provide. While these results are encouraging, further stability tests are required before the inverted pressure can be used with confidence in a simulator model update.

Conclusions. A method for using time-lapse overburden time-shift measurements to invert for reservoir pressure change is presented based on linear elasticity theory. This method as shown uses minimal constraints and is computationally fast and straightforward to implement, when compared with more complex numerical modeling. Results are presented from application of the method to Genesis Field in the Gulf of Mexico. Because of the difficulties of inverting closely spaced vertical layers, we invert for a single equivalent layer. The problem of vertical resolution is one that is consistent for most problems related with turbidites. There is little doubt that the geomechanics of such a reservoir is complex, and we have made several simplifying assumptions; using an equivalent layer to represent three layers does not take account the dilation of the inter-reservoir shales for example. However, despite these assumptions, we find that the inversion method presented here provides results that compare favorably with reservoir simulation predictions, thus lending confidence that this is providing reservoir-scale information that may be used to inform reservoir-management decisions. Many sources of additional data could help constrain this approach. Other hard data may also help to constrain the inversion, in particular downhole deformation measurements and time-lapse acoustic logging and seafloor subsidence and tilt measurements. Other soft constrains might include involving the other components of the strain tensor that are produced as a product of 3D warping (e.g., Hall, 2006), and amplitude data from the reservoir interval as suggested by Corzo and MacBeth (2006) which may also help improve the lateral resolution of the solution.

Suggested reading. "Towards accurate quantitative monitoring of compacting reservoirs using time-lapse seismic" by Corzo and MacBeth (*SEG 2006 Expanded Abstracts*). "A poroelastic reservoir model for predicting subsidence and mapping subsurface pressure fronts" by Du and Olson (*Journal of Petroleum Science and Engineering*, 2001). "Problems of rock mechanics in petroleum engineering" by Geertsma (*International Society of Rock Mechanics*, 1966). "A new technique for pressure-saturation separation from time-lapse seismic: Schiehallion Case Study" by Floricich et al. (*EAGE 2006 Extended Abstracts*). *Petroleum Related Rock Mechanics* by Fjær et al. (Elsevier, 1992). "A methodology for 7D warping and deformation monitoring using time-lapse seismic data" by Hall (GEOPHYSICS, 2006). "Measuring reservoir compaction using time-lapse time shifts" by Hatchell and Bourne (*SEG 2006 Expanded Abstracts*). "In-situ stress dependence of wave velocities in reservoir and overburden rocks" by Holt et al. (*TLE*, 2005). "Preliminary results of the Genesis Field time-lapse seismic project, Gulf of Mexico" by Hudson et al. (OTC paper 18376, 2006). "Measuring velocity sensitivity to production-induced strain at the Ekofisk Field using time-lapse time-shifts and compaction logs" by Janssen et al. (*SEG 2006 Expanded Abstracts*). "Quantitative estimation of compaction and velocity changes using 4D impedance and traveltime changes" by Landrø and Stammeijer (GEOPHYSICS, 2004). "Seismic processing for time-lapse study: Genesis Field, Gulf of Mexico" by Magesan et al. (*TLE*, 2005). "Nuclie of strain in the semi-infinite solid" by Mindlin and Chen (*Journal of Applied Physics*, 1950). "4D time strain and the seismic signature of geomechanical compaction at Genesis" by Rickett et al. (*TLE*, 2007). "Predicting reservoir compaction and casing deformation in deepwater turbidites using a 3D mechanical earth model" by Sayers et al. (SPE paper 103926, 2006). "Induced stresses due to fluid extraction from axisymmetric reservoirs" by Segall (*Pure Applied Geophysics*, 1996). "Note on the stresses produced by a nucleus of strain in a semi-infinite elastic solid" by Sen (*Quarterly Applied Mathematics*, 1951). "Reservoir monitoring with seismic time shifts: Geomechanical modeling for its application to stacked pay" by Schutjens et al. (IPTC paper 10511, 2005). "Using surface deformation to image reservoir dynamics" by Vasco et al. (GEOPHYSICS, 2000). TLE

Acknowledgments: Neil Hodgson acknowledges Chevron ETC and Tom Hudson of the Genesis Asset team for their close collaboration as sponsors of the Edinburgh Time-Lapse Project (ETLP), and Jesus Nunez for useful discussions and providing some figures. We also thank the ETLP-sponsoring companies: BG Group, BP, Chevron, ConocoPhillips, ExxonMobil, Ikon Science, Landmark, Maersk, Norsor, Hydro, Petrobras, Shell, Statoil, Total, and Woodside.

Corresponding author: Neil.Hodgson@pet.hw.ac.uk